Raft-like microdomains play a key role in mitochondrial impairment in lymphoid cells from patients with Huntington's disease

Laura Ciarlo,[1,*] **Valeria Manganelli,**[1,†] **Paola Matarrese,**[*,§] **Tina Garofalo,**[†] **Antonella Tinari,**[**] **Lucrezia Gambardella,**[*] **Matteo Marconi,**[*] **Maria Grasso,**[†] **Roberta Misasi,**[†] **Maurizio Sorice,**[2,†] **and Walter Malorni**[2,3,*,††]

Section of Cell Aging and Degeneration, Department of Therapeutic Research and Medicine Evaluation,[*] and Department of Technology and Health,[**] Istituto Superiore di Sanità, Rome, Italy; Department of Experimental Medicine,[†] "Sapienza" University, Rome, Italy; Center of Integrated Metabolomics,[§] Rome, Italy; and San Raffaele Institute Sulmona,[††] L'Aquila, Italy

Abstract Huntington's disease (HD) is a genetic neurodegenerative disease characterized by an exceedingly high number of contiguous glutamine residues in the translated protein, huntingtin (Htt). The primary site of cell toxicity is the nucleus, but mitochondria have been identified as key components of cell damage. The present work has been carried out in immortalized lymphocytes from patients with HD. These cells, in comparison with lymphoid cells from healthy subjects, displayed: *i*) a redistribution of mitochondria, forming large aggregates; *ii*) a constitutive hyperpolarization of mitochondrial membrane; and *iii*) a constitutive alteration of mitochondrial fission machinery, with high apoptotic susceptibility. Moreover, mitochondrial fission molecules, e.g., protein dynamin-related protein 1, as well as Htt, associated with mitochondrial raft-like microdomains, glycosphingolipid-enriched structures detectable in mitochondria.▐▐ These findings, together with the observation that a ceramide synthase inhibitor and a raft disruptor are capable of impairing the peculiar mitochondrial remodeling in HD cells, suggest that mitochondrial alterations occurring in these cells could be due to raft-mediated defects of mitochondrial fission/fusion machinery.—Ciarlo, L., V. Manganelli, P. Matarrese, T. Garofalo, A. Tinari, L. Gambardella, M. Marconi, M. Grasso, R. Misasi, M. Sorice, and W. Malorni. **Raft-like microdomains play a key role in mitochondrial impairment in lymphoid cells from patients with Huntington's disease.** *J. Lipid Res.* **2012. 53: 2057–2068.**

Supplementary key words rafts • mitochondria • fission • huntingtin

Huntington's disease (HD) is a genetic neurodegenerative disease that is seemingly due to the expansion of a trinucleotide repeat in the IT15 gene. This results in an exceedingly high number of contiguous glutamine residues in the translated protein, huntingtin (Htt) (1). The disease can occur in homozygous and heterozygous patients carrying the same CAG expansion length, but despite a similar age at onset, it progresses more rapidly in the homozygote (2).

The primary site of cell toxicity is the nucleus (3). Mitochondria have, however, been identified as key components of the series of events leading to cell injury (4). For instance, recent studies in animal models highlighted a direct mitochondrial toxicity that may specifically contribute to the occurrence of the clinical phenotype (5). The key role of mitochondrial dysfunction seems to be due, or to be associated with, the accumulation of mutant Htt fragments at the mitochondrial membrane (6, 7). This suggested that the mechanisms of cell death that lead to the progression of the disease could rely on metabolic impairment. In fact, accordingly, it has been hypothesized that cell loss as a pathogenic mechanism of HD could be due to disturbances of cell death pathways. Both apoptosis and autophagy have been taken into account (8, 9). Apoptosis, the programmed process of cell death associated with the activation of specific proteases, i.e., caspases, and involving mitochondria-mediated release of apoptogenic factors, appears as pivotal. Autophagy, a tentative cytoprotection pathway of the cell also leading to cell death as final event, appeared involved as well (10).

In the present study, on the basis of data in the literature (6, 11, 12), we focused on the possible role of mitochondrial features in lymphoblastoid cell lines obtained from HD patients. In particular, we analyzed the implication of the mitochondrial raft-like microdomains (13) in the above-described processes. In these dynamic structures, some molecules, including gangliosides (GD3, GM3), low levels of cholesterol, the voltage-dependent anion channel-1 (VDAC-1), and the fission protein hFis1, are constitutively present. By contrast, in T cells, some proteins of the Bcl-2 family (i.e., truncated Bid, t-Bid, and Bax) as well as protein dynamin-related protein 1 (Drp1) are recruited to these mitochondrial raft-like microdomains only upon CD95/Fas triggering (13). These are glycosphingolipid-enriched structures, which can participate in the apoptotic cascade, being recruited to the mitochondria under pro-apoptotic stimulation. In particular, it has been hypothesized that lipid raft recruitment to the mitochondria could have a role in the morphogenetic changes leading to organelle fission, a prerequisite for apoptosis execution (14, 15). In the present work we report that the high susceptibility to apoptosis of lymphoid cells from HD patients is associated with raft-mediated defects in mitochondrial fission machinery.

MATERIALS AND METHODS

Cells and treatments

Human lymphoblastoid cells from healthy subjects (HS) and HD patients were acquired from Coriell Institute for Medical Research (Camden, NJ). Epstein-Barr virus immortalized cell lines included two unexpanded normal cells from HS, here considered as controls, and two cell lines from HD patients with highly expanded CAG repeats (70–120). Superimposable results were obtained with the two cell lines from HS and with those obtained from HD patients. Cells were maintained in RPMI 1640 medium (both Gibco-BRL, Life Technologie) containing 20% fetal calf serum (FCS) plus 100 U/ml penicillin, 100 mg/ml streptomycin, at 37°C in a humified 5% CO_2 atmosphere.

Apoptosis was induced by incubating cells at a concentration of 5×10^5 per ml by adding 1 mM staurosporin (STS) (Sigma-Aldrich) for 2 h at 37°C. To analyze the effect of sphingolipid depletion or raft alteration on STS-induced cell death, cells were pretreated with 30 µM fumonisin B1 (FB1) (Sigma) (inhibitor of ceramide synthase) for 24 h or 2 mM methyl-β-cyclodextrin (MBC) (Sigma) (lipid raft disruptor that removes cholesterol from membranes) for 20 min at 37°C. After treatments, cells were collected and prepared for the experimental procedures described below.

Cell death assays

Quantitative evaluation of apoptosis was performed by flow cytometry after double staining using FITC-conjugated annexin V/Trypan blue (Eppendorf), which allows discrimination among early apoptotic, late apoptotic, and necrotic cells.

Flow cytometry analysis of the redox balance

Cells (5×10^5) were incubated with 1 µM of dihydroethidium (DHE) (Molecular Probes) for superoxide anion detection (16). After 20 min at 37°C, cells were washed and immediately analyzed on a cytometer.

Electron microscopy

For transmission electron microscopy (TEM) examination, human lymphoblastoid cells from HS and HD patients were fixed in 2.5% cacodylate-buffered (0.2 M, pH 7.2) glutaraldehyde for 20 min at room temperature and postfixed in 1% OsO_4 in cacodylate buffer for 1 h at room temperature. Fixed specimens were dehydrated through a graded series of ethanol solutions and embedded in Agar 100 (Agar Aids) (13). Serial ultrathin sections were collected on 200-mesh grids and then counterstained with uranyl acetate and lead citrate. Sections were observed with a Philips 208 electron microscope at 80 kV (Philips Co.).

Immunoelectron microscopy

Thin sections from HS and HD cells were collected on gold grids, treated with PBS containing 1% (w/v) gelatin, 1% BSA, 5% FCS, and 0.05% Tween 20 and then incubated with anti-Htt polyclonal antibody (Cell Signaling) diluted 1:10. After washing for 1 h at room temperature, unstained sections were labeled with goat-anti-rabbit IgG-gold conjugate 10 nm (1:10) for 1 h at room temperature. Negative controls were incubated with the gold-conjugate alone (15). A quantification of gold particles was also carried out by evaluating at the electron microscopy at least 20 different fields at high magnification (20,000×) and analyzing at least 50 cells on different grids. Gold particles in the cell cytoplasm or associated with mitochondria were evaluated. Results obtained are expressed as mean ± standard deviation of gold particles per cell.

Mitochondrial membrane potential in living cells

The mitochondrial membrane potential (MMP) of controls and treated cells was studied by using 5-5′,6-6'-tetrachloro-1,1',3,3′-tetraethylbenzimidazol-carbocyanine iodide (JC-1) (Molecular Probes) probe. In line with this method, living cells were stained with 10 µM of JC-1, as previously described (17). Tetramethylrhodamine ester 1 µM (Molecular Probes, red fluorescence) was also used to confirm data obtained by JC-1.

Sucrose-gradient fractionation

Lipid raft fractions from lymphoid cells derived from HD patients or HS were isolated as previously described (13). Briefly, cell lysates were centrifuged for 5 min at 1,300 g. The supernatant fraction (postnuclear fraction) was subjected to linear sucrose density gradient (5–30%) centrifugation. After centrifugation, the gradient was fractionated, and 11 fractions were collected starting from the top of the tube. The fraction samples were loaded by volume.

Immunoblotting analysis of fractions

All the fractions, obtained as reported above, were subjected to SDS-PAGE. The proteins were electrophoretically transferred onto PVDF membranes (Bio-Rad) and probed with anti-hFis1 polyclonal antibody (Alexis Biochemicals, L17449/d), anti-OPA1 monoclonal antibody (BD Biosciences Pharmingen, clone 18), anti-Drp1 monoclonal antibody (BD Biosciences Pharmingen, clone 8), anti-Bak polyclonal antibody (Santa Cruz Biotechnology, clone G-23, sc-832), anti-Bax monoclonal antibody (Santa Cruz Biotechnology, clone N-20 sc:493), anti-Bid polyclonal antibody (R&D Systems, Inc.), or anti-Htt polyclonal antibody (Cell Signaling Technology). Bound antibodies were visualized with HRP-conjugated anti-rabbit IgG or anti-mouse IgG (Sigma), and immunoreactivity was assessed by chemiluminescence reaction, using the ECL Western detection system (Amersham Biosciences). Densitometric scanning analysis was performed by Mac OS X (Apple Computer International), using NIH Image 1.62 software. The density of each band in the same gel was analyzed, values were

totaled, and then the percent distribution across the gel was detected.

Preparation of fractions from mitochondria

Lymphoid cells from HD patients or HS were collected by centrifugation. Mitochondria were isolated as previously reported (18). After evaluation of the protein concentration by Bradford Dye Reagent assay (Bio-Rad), mitochondria fractions were analyzed by Western blot analysis using the anti-Htt polyclonal antibody (Cell Signaling), as reported above. The purity of mitochondrial preparations was assessed by Western blot by checking the subunit IV of cytochrome c oxidase (COX-IV), using anti-COX-IV monoclonal antibody (Molecular Probes).

Alternatively, mitochondria were detergent-solubilized according to Skibbens et al. (19). Briefly, mitochondria were lysed with 1 ml of extraction buffer (25 mM HEPES, pH 7.5, 0.15 NaCl, 1% Triton X-100, and 100 kallikrein U/ml aprotinin) for 20 min on ice. Lysates were collected and centrifuged for 2 min in an ALC microfuge at 12,000 rpm at 4°C. Sovranatants, containing Triton X-100-soluble material, were collected; pellets were subjected to a second centrifugation (30 s) in order to remove the remaining soluble material. The pellets were then solubilized in 100 μl of buffer containing 50 mM Tris-HCl, pH 8.8, 5 mM EDTA, and 1% SDS. DNA was sheared by passage through a 22 gauge needle. Both Triton X-100-soluble and -insoluble material were analyzed by Western blot as described above by checking Htt using a specific anti-Htt polyclonal antibody (Cell Signaling).

TLC immunostaining analysis

Briefly, Triton X-100-soluble and -insoluble fractions from mitochondria were extracted twice in chloroform-methanol-water (4:8:3) (v/v/v) and subjected to Folch partition by the addition of water, resulting in a final chloroform-methanol-water ratio of 1:2:1.4 The upper phase, containing polar glycosphingolipids, was purified of salts and low-molecular-weight contaminants using Bond Elut C18 columns (Superchrom). The eluted glycosphingolipids were dried down and separated by high-performance TLC, using aluminum-backed silica gel 60 (20 × 20) plates (Merck, Darmstadt). Chromatography was performed in chloroform-methanol-0.25% aqueous KCl (5:4:1) (v/v/v). The dried chromatograms were soaked for 90 s in a 0.5% (w/v) solution of poly(iso)bytyl methacrylate beads (Polysciences) dissolved in hexane. The plates were immunostained for 1 h at room temperature with GMR19 anti-GD3 MoAb (Seikagaku Corp.) and then with HRP-conjugated anti-mouse IgM (Sigma Chemical Co.). Immunoreactivity was assessed by chemiluminescence reaction, using the ECL Western detection system (Amersham Biosciences) (20).

Immunofluorescence analysis

Cells were stained with MitoTracker-Red 1 μM (Molecular Probes) for 45 min at 37°C. After washing in PBS, cells were fixed and permeabilized as stated elsewhere (14). Samples were incubated with anti-Drp1 polyclonal antibody (Santa Cruz Biotechnology) for 1 h at 4°C, followed by Alexa Fluor 488-conjugated anti-mouse IgG (Molecular Probes). Alternatively, fixed and permeabilized cells were incubated with anti-Drp1 polyclonal antibody (Santa Cruz Biotechnology), followed by incubation with AlexaFluor 488-conjugated anti-rabbit IgG for an additional 30 min. After the washings, cells were incubated for 1 h at 4°C with anti-GD3 monoclonal antibody (Seikagaku), followed by AlexaFluor 594-conjugated anti-mouse IgM (Molecular Probes). All samples were counterstained with Hoechst 33342, mounted with glycerol-PBS (2:1), and analyzed by using an Olympus fluorescence microscope (Olympus Corporation).

Data analysis and statistics

All samples were analyzed with a FACSCalibur cytometer (BD) equipped with a 488 argon laser and 633 visible red diode laser. At least 20,000 events were acquired. Data were recorded and statistically analyzed by a Macintosh computer, using CellQuest-Pro Software. Statistical analysis of apoptosis data and morphometric analysis were performed by using Student's t-test or one-way variance analysis by using Prism program (version 4) by GraphPad for Macintosh. All data reported were verified in at least three different experiments and reported as mean ± SD. Only P values of less than 0.01 were considered as statistically significant.

RESULTS

Analysis of apoptosis, reactive oxygen species, and mitochondrial membrane potential

We first compared the apoptotic susceptibility of lymphoid cells from HD patients with that of lymphoid cells from HS. In particular, we evaluated: i) annexin V cell positivity, ii) reactive oxygen species (ROS) generation, and iii) mitochondrial membrane potential. We used staurosporin (STS) as a representative pro-apoptotic stimulus known in the literature as an inducer of ROS production and mitochondria-mediated cell death (21). As far as apoptosis was concerned, we found that lymphoid cells from HD patients displayed significantly higher levels of "spontaneous apoptosis" with respect to those from HS and that they were significantly more susceptible to STS-mediated apoptosis (**Fig. 1A**). Accordingly, we found a significant difference in ROS production between cells from HD patients and HS, either untreated (basal conditions) or after STS administration (Fig. 1B). Because mitochondria are thought to be the target and the source of ROS, we evaluated in our experimental system the possible changes of MMP, a key event in mitochondrial homeostasis maintenance (22). Data obtained by flow cytometry analysis were in line with the above results (Fig. 1C). In fact, it is well known that MMP alterations are associated with apoptosis proneness or execution. In particular, an increase of MMP, i.e., hyperpolarization of MM (MMH), has been found to be a determinant in apoptotic susceptibility (23), whereas mitochondrial membrane depolarization (MMD) represents a "point of no return" in the apoptosis execution (24). In our experimental model of HD, we found that independently of any treatment, a hyperpolarization of mitochondrial membrane (MM) was detectable in a significantly higher percentage of cells from HD patients in comparison to cells from HS (Fig. 1C, black and gray full bars, respectively). After treatment with STS, according to apoptosis data (Fig. 1A), the percentage of cells with MMD was significantly higher in cells from HD patients than in cells from HS (Fig. 1C, black and gray empty bars, respectively).

Mitochondrial features

The results reported above were further supported by TEM analyses (**Fig. 2**). Ultrastructural studies showed the following: in the absence of any pro-apoptotic stimulation,
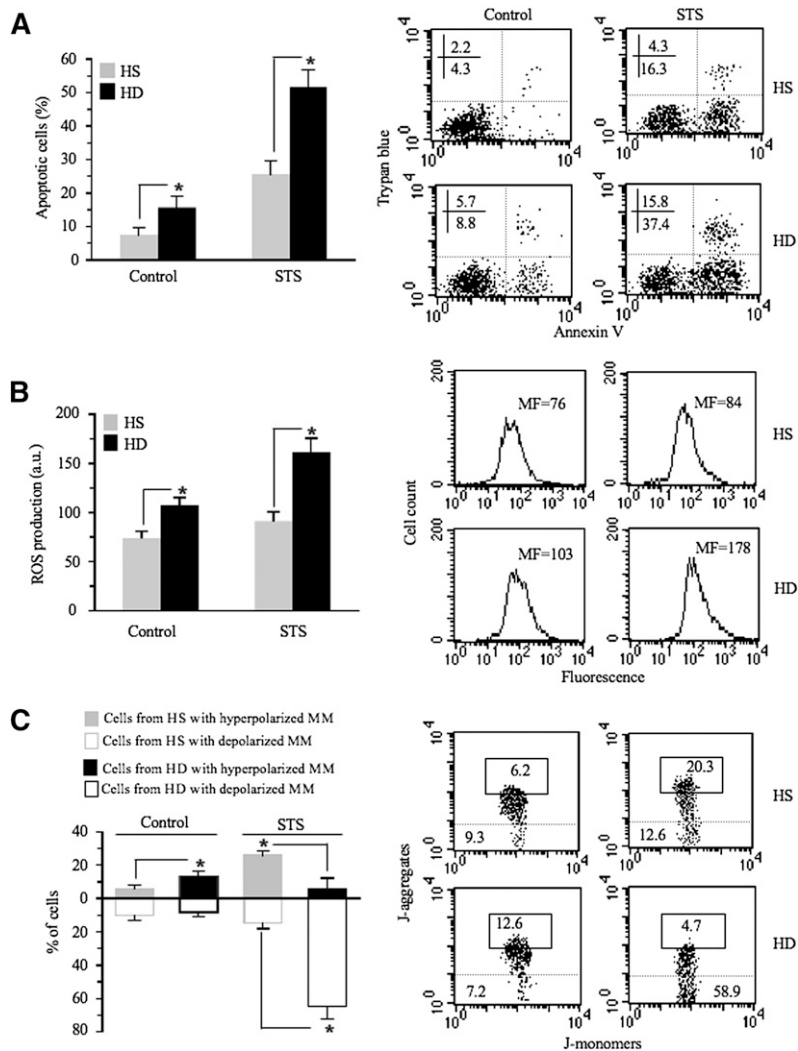
Fig. 1. Analysis of apoptosis, ROS, and mitochondrial membrane potential. A: Biparametric flow cytometry analysis of apoptosis after double staining of cells with annexin V-FITC/Trypan blue. In the left panel, bar graph shows the results obtained from three independent experiments reported as mean ± SD. * $P < 0.01$. In the right panels, dot plots from a representative experiment are shown. Numbers represent the percentage of annexin V single-positive cells (early apoptosis, lower right quadrant) or annexin V/Trypan blue double-positive cells (late apoptosis, upper right quadrant). B: Cytofluorimetric analysis of superoxide anion production. Values reported represent the median fluorescence. In the left panel, bar graph reporting the mean of the results obtained from four independent experiments ± SD is shown. * $P < 0.01$. In the right panels, results obtained in a representative experiment are shown as fluorescence emission histograms. C: Biparametric flow cytometry analysis of MMP after staining with JC-1. In the left panel, bar graph shows the results obtained from three independent experiments reported as mean ± SD. Full (gray or black) and empty columns represent the percentages of cells with hyperpolarized or depolarized mitochondrial membranes, respectively. * $P < 0.01$. To note that independently of any treatment, a MMH was detectable in a significantly higher percentage of cells from HD patients in comparison to cells from HS (black and gray bars, respectively). After treatment with STS, according to apoptosis data (see Fig. 1A), the percentage of cells with MMD was significantly higher in cells from HD patients than in cells from HS (empty columns). In the right panels, dot plots from a representative experiment are shown. Numbers reported in the boxed area represent the percentages of cells with hyperpolarized mitochondria. In the area under the dotted line, the percentage of cells with depolarized mitochondria is reported.

mitochondria were often redistributed (clustered and/aggregated) at one pole of the cells from HD patients (Fig. 2A). In particular, mitochondria displayed marked electrondensity and coalescence (Fig. 2B). Under apoptotic stimulation, HD cells undergoing apoptosis showed bolstered mitochondrial structural alterations, with the formation of large bundles of packed mitochondria (Fig. 2C, D). "Normal" mitochondrial morphology in intact cells from HS and typical features of apoptosis in STS-treated cells from HS are shown in Fig. 2E, F.

Localization of Htt in mitochondrial raft-like microdomains

A preliminary analysis was performed to clarify whether mutated Htt may be present in lipid microdomains. Sucrose gradient fraction preparation (**Fig. 3A**) and related densitometric analysis (Fig. 3B) clearly displayed the presence of mutated Htt in buoyant low-density detergent-resistant fractions (i.e., fractions 5–6) of cells from HD patients only. These fractions correspond to lipid microdomains (13).

A recent hypothesis is that the mutated Htt impairs mitochondrial function, resulting in increased oxidative stress and consequent cytotoxicity. Several lines of evidence

support the notion that energy production impairment and mitochondrial dysfunction play a key role in the pathogenesis of HD (25). According to this, we found that Htt was associated with the mitochondrial fraction in cells from HD patients but not in cells from HS (Fig. 3C). In fact, analysis of crude mitochondria preparations obtained from HD and HS lymphoid cells, subjected to 3–8% Tris-acetate gradient gel electrophoresis, revealed a 340 kDa positive band, detected by anti-Htt polyclonal antibody (Fig. 3C, top panel) in HD cells but not in HS cells.

Furthermore, to demonstrate that Htt was present in mitochondrial raft-like microdomains, we performed the same analysis in both Triton X-100-insoluble and -soluble fractions, obtained from mitochondria from the same cells. The analysis revealed that Htt was almost completely recruited to Triton X-100-insoluble fractions in HD cells, corresponding to raft-like microdomains (20), whereas it was absent in mitochondrial preparations from HS (Fig. 3C, bottom panel). Moreover, we analyzed the distribution of GD3, a paradigmatic ganglioside component of raft-like microdomains (13). As expected, it was present almost exclusively in the insoluble fractions, confirming the presence of ganglioside molecules in mitochondrial raft-like microdomains of lymphoid cells from HD patients.
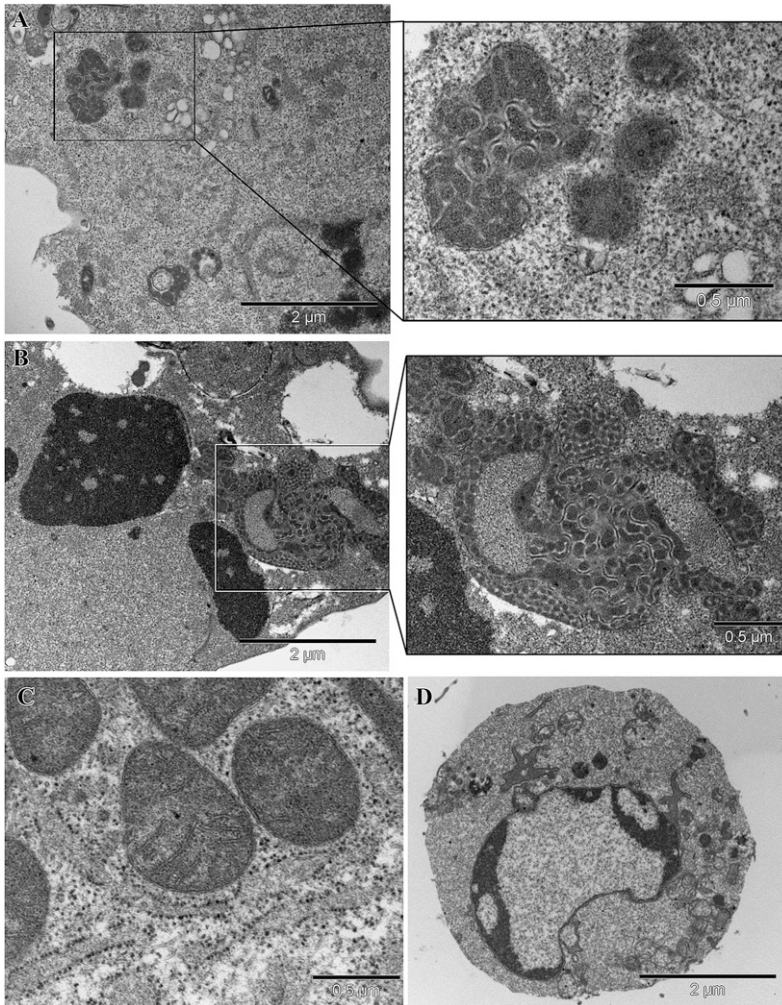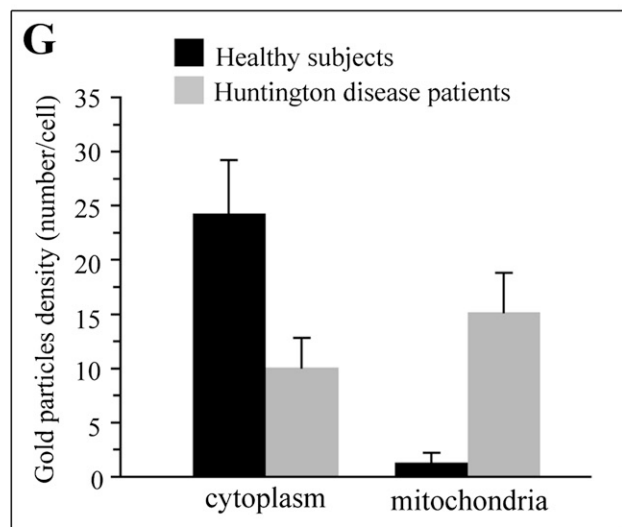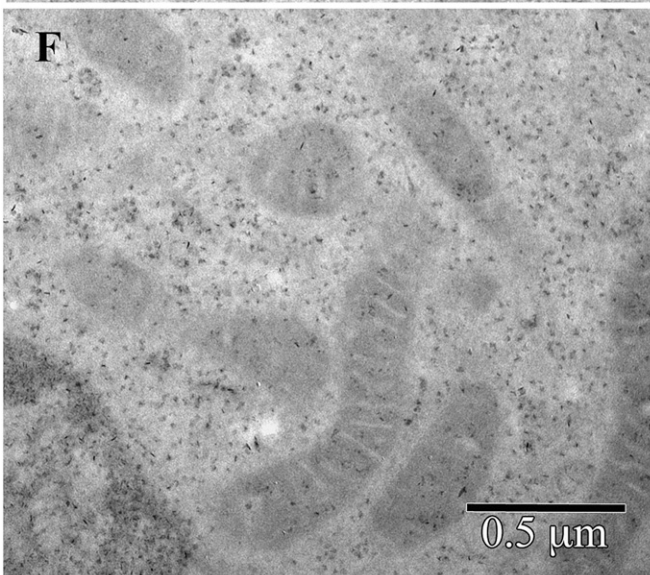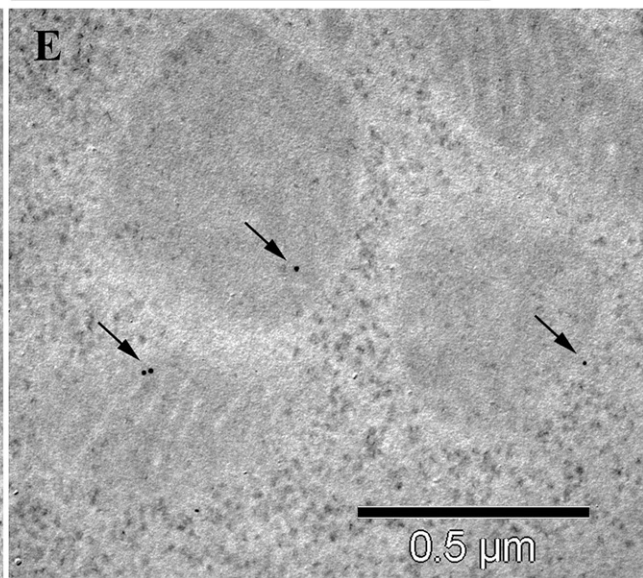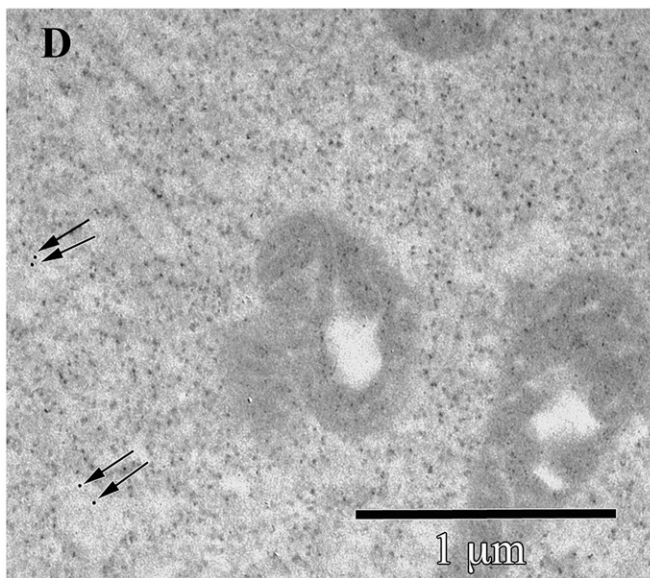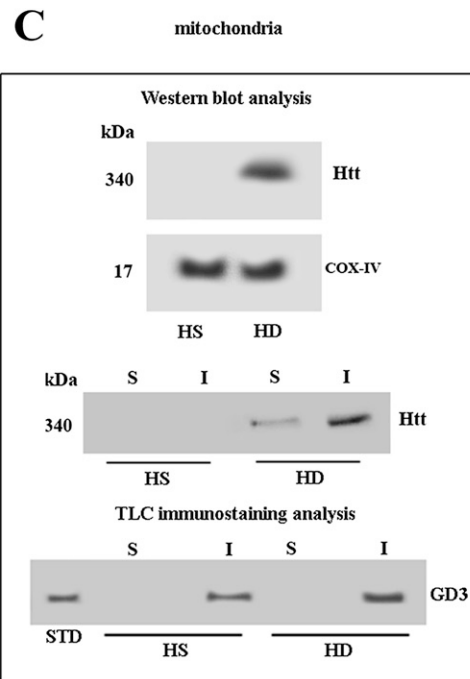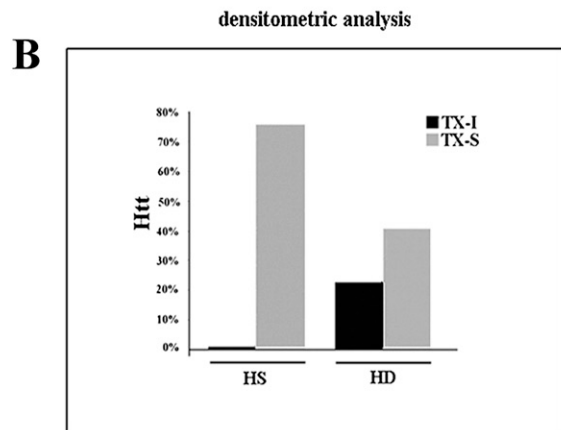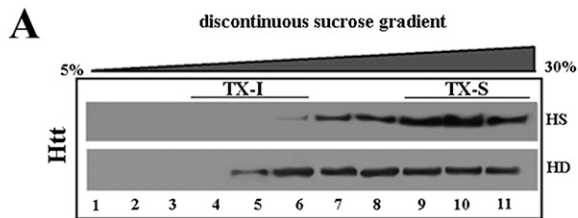
Fig. 2. Mitochondrial features. A: At the ultrastructural level, mitochondria from HD cells appeared as electron-dense, coalescent organelles forming aggregates at one pole of the cell (inset and upper right panel). B: After treatment with STS, cells from HD patients showed chromatin aggregation typical of apoptosis as well as bolstered mitochondrial structural alterations characterized by the formation of large bundles (inset and middle right panel). C: Normal mitochondria from HS lymphoid cells. D: Control lymphoid cell undergoing apoptosis.

Transmission immunoelectron microscopy confirmed this association. In fact, gold particles labeling Htt, which, as expected, is poorly expressed in lymphoid cells, were barely detectable in the cell cyoplasm but substantially undetectable as associated with mitochondria in control cells from HS (Fig. 3D). By contrast, gold particles were often visible in close contact with mitochondria in sections from cells from HD patients (Fig. 3E; a representative micrograph obtained from negative controls, i.e., gold labeling without primary antibody, is shown in Fig. 3F). Morphometric analyses carried out on these sections indicated that *i*) as expected, few gold particles were detectable either in sections of lymphoid cells from HS (control samples) or in sections of cells from HD patients. However, *ii*) HD cells displayed gold labeling of Htt associated with mitochondria. In particular, quantitative evaluation of each cell at the EM indicated that in cells from HS, gold particles labeling Htt, distinguishable from ribosomes for their regular shape and their electrodensity, were few and scattered through the cell cytoplasm (mean value: 24 ± 5 particles per cell), whereas gold particles were substantially undetectable in close proximity of mitochondria (mean value: 1 ± 1 per cell). By contrast, in cells from HD patients, gold particles detectable in the cell cytoplasm were significantly less than in sections from HS (mean

value: 10 ± 2 per cell, $P < 0.01$), whereas gold particles visible as associated with mitochondria were significantly more than in HS (mean value: 14 ± 3 per cell, vs. 1 ± 1, $P < 0.01$; see histogram in Fig. 3G).

Bcl-2 family pro-apoptotic proteins

We investigated whether mitochondrial raft-like microdomains were directly involved in the mechanism leading to the high susceptibility of HD cells to apoptosis. With this aim, we primarily focused on the Bcl-2 family death promoters Bak, Bax, and Bid, which represent indispensable effectors of the mitochondrial-mediated apoptotic pathway. We analyzed the distribution of these proteins in fractions obtained by a 5–30% discontinuous sucrose gradient. As shown in **Fig. 4**, in cells from HS, Bak was present in fractions 6–11 and Bax in fractions 7–11, but both proteins were virtually absent in the fractions corresponding to raft-like microdomains. By contrast, in cells from HD patients, either Bak or Bax appeared almost completely restricted at buoyant low-density detergent-resistant fractions (4–6). Furthermore, we analyzed the distribution of Bid, a proapoptotic protein of the Bcl-2 family that acts directly on mitochondrial membranes to facilitate the release of apoptogenic factors. Bid, as full-length protein, was almost entirely present in Triton X-100 soluble fractions

A discontinuous sucrose gradient

5%   30%

TX-I   TX-S

Htt   HS

                                                    HD

1   2   3   4   5   6   7   8   9   10   11

B densitometric analysis

C mitochondria

Western blot analysis

kDa

340   Htt

17   COX-IV

        HS   HD

kDa   S   I   S   I

340   Htt

        HS   HD

TLC immunostaining analysis

        S   I   S   I

                                       GD3

STD   HS   HD

of cells from HS (Fig. 4). Conversely, in cells from HD patients, Bid was processed into the active form (truncated-Bid, t-Bid), which was present in the buoyant low-density Triton X-100-resistant fractions only. Thus, in cells from HD patients, the active form of Bid, i.e., t-Bid, is constitutively recruited to the buoyant low-density Triton X-100-resistant fraction.

Furthermore, to confirm that the Bcl-2 family death promoters Bak, Bax, and Bid were present in mitochondrial raft-like microdomains, we performed the same analysis in both Triton X-100-insoluble and -soluble fractions, obtained from mitochondria from the same cells, according to Malorni et al. (20). The analysis of these samples revealed that Bak, Bax, and t-Bid were almost completely recruited to Triton X-100-insoluble fractions, corresponding to raft-like microdomains, in lymphoid cells from HD patients.

Mitochondrial fission machinery

It has recently been hypothesized that mitochondrial fission can sensitize cells to apoptosis induction. In addition, mitochondria remodeling in terms of structural modifications, i.e., their curvature changes, as well as their fission process, could be under the influence of several molecules, including lipid microdomains (13). We thus analyzed the possible localization of fission proteins both in buoyant low-density Triton X-100-resistant fractions. As shown in **Fig. 5A**, the analysis of the distribution of hFis1 and OPA1, two molecules involved in the mitochondrial fission machinery (26, 27), revealed that in cells from HD patients, these proteins were detectable in fractions 4–11 (hFis1) and 5–11 (OPA1). Hence, at variance with cells from HS, in cells from HD patients, both OPA1 and hFis1 were found in fractions corresponding to raft-like microdomains (Fig. 5A, compare first lanes with second lanes in upper and central panels; in Fig. 5B the corresponding densitometric analyses). Important findings were detected as far as Drp1 was concerned. This is a further key molecule involved in mitochondrial fission (28), and it is normally recruited to mitochondrial raft-like microdomains only under apoptotic stimulation (14, 15). Strikingly, we found that it was almost entirely restricted to Triton X-100-soluble fractions in cells from HS (Fig. 5A, first lane in bottom panel), whereas it was also detected in the buoyant low density detergent-resistant fractions in cells from HD

patients (Fig. 5B, second lane in bottom panel; in Fig. 5B, corresponding densitometric analyses). This indicates that in HD cells, Drp1 was constitutively localized in mitochondrial raft-like microdomains. Furthermore, to confirm that hFis, OPA1, and Drp1 were present in mitochondrial raft-like microdomains, we performed the same analysis in both Triton X-100-insoluble and -soluble fractions, obtained from mitochondria. The analysis of these samples revealed that hFis1 and OPA1 were highly enriched in Triton X-100-insoluble fractions, whereas Drp1 was recruited to Triton X-100-insoluble fraction, corresponding to raft-like microdomains, in lymphoid cells from HD patients (Fig. 5C).

The immunofluorescence analysis (Fig. 5D) indicated a preferential mitochondrial localization of Drp1 in HD samples (right panel) whereas in the HS sample, Drp1 was mostly ditributed in the cytoplasm. In agreement with the above biochemical data, Drp1 showed an evident colocalization with GD3 in cells from HD patients only (left panel).

Mitochondrial raft-like microdomains and apoptotic susceptibility

On the basis of the results reported above, we assessed the implication of raft-like microdomains in the HD cell susceptibility to mitochondria-mediated apoptosis. With this aim, two different agents capable of perturbating microdomain integrity have been considered: FB1, a ceramide synthase inhibitor (29, 30), and MBC, a raft disruptor (13, 31). We found that either FB1 or MBC, when administered before STS treatment, were capable of significantly hindering apoptosis in HS as well as in HD cells (**Fig. 6A**, compare with values found in HS and HD cells treated with STS alone, represented by dotted and dashed lines, respectively). Accordingly, FB1 and MBC significantly reduced apoptosis-associated ROS production (Fig. 6B; compare with values found in HS and HD cells treated with STS alone, represented by dotted and dashed lines, respectively). Interestingly, these two compounds also reduced mitochondrial aggregation (when analyzed by TEM, not shown), the mitochondrial membrane hyperpolarization (Fig. 6C) (which was detectable in HD cells independently of any treatment, see Fig. 1C), or the loss of MMP that follows STS treatment (Fig. 6C, compare with

---

Fig. 3. Localization of Htt at mitochondrial raft-like microdomains. **A**: Western blot analysis of sucrose gradient fractions. Cells from HD patients or from HS were lysed, and the supernatant fraction was subjected to sucrose density gradient. After centrifugation, the gradient was fractioned, and each gradient fraction was recovered and analyzed by Western blot using an anti-Htt polyclonal antibody. B: Densitometric analysis of sucrose gradient fractions. The columns indicate the percent distribution across the gel of fractions 4, 5, and 6 (buoyant low-density TX-100-resistant fractions, TX-I) and 9, 10, and 11 (TX-100-soluble fractions, TX-S), as detected by densitometric scanning analysis. C: Mitochondria from HD or HS cells were analyzed by Western blot and probed with anti-Htt polyclonal Ab or with anti-COX-IV MoAb. Mitochondria from HD or HS cells were solubilized by detergent as reported in Materials and Methods. Both Triton X-100-soluble (S) and -insoluble (I) fractions were analyzed by Western blot and probed with anti-Htt polyclonal Ab. Alternatively, Triton X-100-soluble (S) and -insoluble (I) fractions from mitochondria were subjected to ganglioside extraction. The extracts were run on high-performance TLC aluminum-backed silica gel and were analyzed for the presence of GD3 by TLC immunostaining analysis, using an anti-GD3 MoAb (GMR19). D–F: Transmission immunoelectron micrographs (without uranyl acetate-lead citrate counterstaining). In cells from HS, gold particles labeling Htt were very few and dispersed in the cytoplasm (arrows in D). In cells from HD patients, gold particles were detectable at the mitochondrial level (arrows in E). A representative micrograph of negative control samples stained only with gold-conjugated secondary antibody is shown in F. Results of morphometric evaluations of gold particles detected in the cytoplasm or associated with mitochondria are shown in G. Note the significant difference in the presence of cytoplasmic and mitochondria-associated gold particles between lymphoblastoid cells from HS and HD patients.
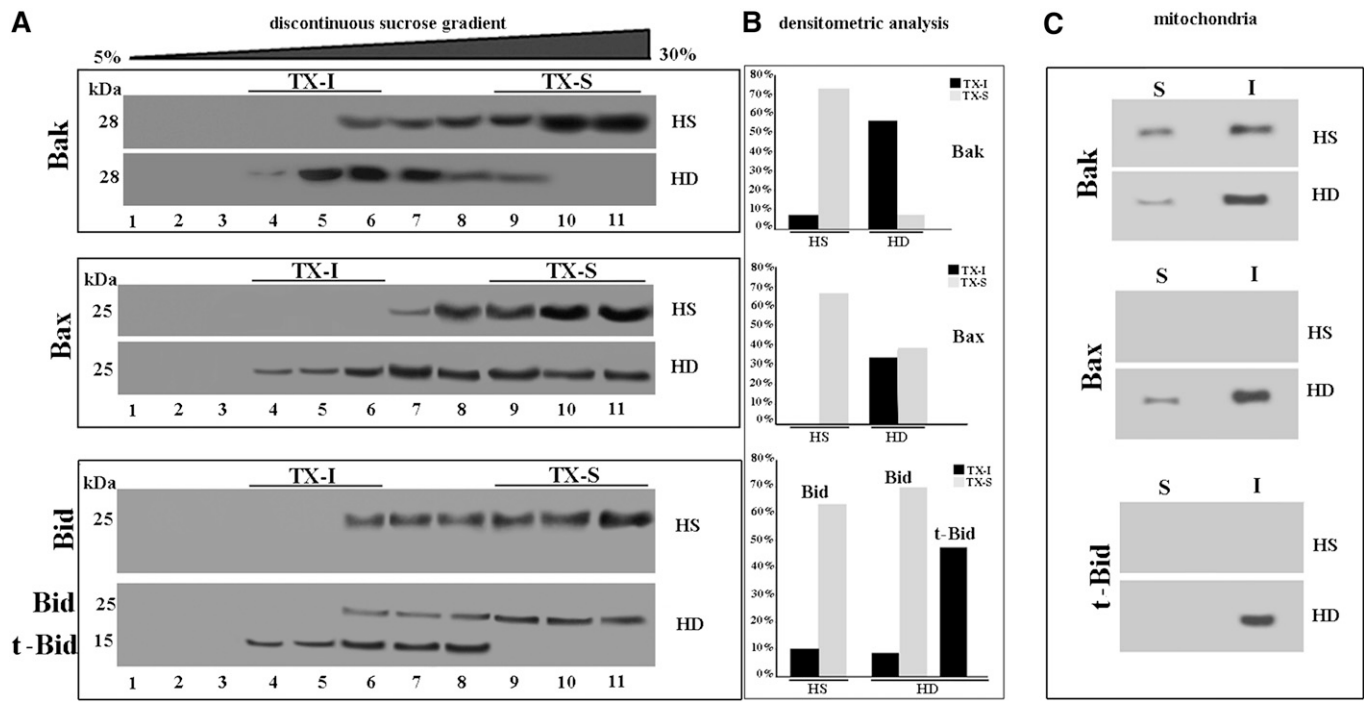
Fig. 4. Bcl-2 family pro-apoptotic proteins. A: Western blot analysis of sucrose gradient fractions. Cells from HD patients or HS were lysed, and the supernatant fraction was subjected to sucrose density gradient. After centrifugation, the gradient was fractioned and each gradient fraction was recovered and analyzed by Western blot. First line: fractions obtained after sucrose density gradient, either HS or HD cells, were analyzed using an anti-Bak polyclonal Ab. Second line: fractions obtained after sucrose density gradient, either HS or HD cells, were analyzed using an anti-Bax monoclonal Ab. Third line: fractions obtained after sucrose density gradient, either HS or HD cells, were analyzed using an anti-Bid polyclonal Ab. B: Densitometric analysis of sucrose gradient fractions. The columns indicate the percent distribution across the gel of fractions 4, 5, and 6 (buoyant low-density TX-100-resistant fractions, TX-I) and 9, 10, and 11 (TX-100-soluble fractions, TX-S), as detected by densitometric scanning analysis. C: Mitochondria from HD or HS cells were detergent solubilized as reported in Materials and Methods. Both Triton X-100-soluble (S) and -insoluble (I) fractions were analyzed by Western blot and probed with anti-Bak polyclonal Ab, anti-Bax MoAb, or anti-Bid polyclonal Ab. The fraction samples were loaded by volume.

values found in HS and HD cells treated with STS alone, represented by dotted and dashed lines, respectively).

DISCUSSION

In the present work we analyzed the peculiar cell model represented by immortalized lymphocytes from patients with HD. These cells, in comparison with their "normal" counterparts (lymphoid cells from HS), displayed some important differences: *i*) a constitutive disparity in ROS/ reactive nitrogen species (RNS) generation and mitochondrial structural features, and *ii*) a higher susceptibility to mitochondria-mediated apoptosis. Investigating the subcellular mechanisms of this behavior, we found some striking findings in these cells: *i*) a constitutive *hyper*polarization of mitochondrial membrane and a redistribution of mitochondria forming large aggregates, *ii*) a constitutive relocalization of mitochondrial fission machinery at the mitochondria raft-like domains, and *iii*) an association of Htt with mitochondrial raft-like microdomains. We hypothesize that these domains could play a role in the metabolic dysfunction found in lymphoid cells from HD patients.

The mechanisms underlying cell death by apoptosis bring into play a series of morphogenetic changes of mitochondria that contribute to the execution of the death program of the cell. This mitochondria remodeling and redistribution in the cell cytoplasm precedes the alteration of the mitochondrial membrane potential, i.e., MMH, the rearrangement of the organelles in the cell cytoplasm, and their fission, i.e., their division and fragmentation. Thereafter, apoptogenic factors released by mitochondria lead to the apoptosis execution pathway. It has recently been demonstrated that mitochondrial fragmentation and cristae alterations characterize cellular models of HD and participate in their increased susceptibility to apoptosis (32). Furthermore, very recently, genotype- and time-dependent caspase activity abnormalities have been demonstrated in blood cells from HD patients (33). In particular, recent literature on this argument claims that mutant Htt can interact with the mitochondrial Drp1, enhancing GT-Pase Drp1 enzymatic activity and causing excessive mitochondrial fragmentation and abnormal distribution (32, 33). In neurons, it can lead to defective axonal transport of mitochondria and selective synaptic degeneration (34, 35). On the basis of our results, we add a key actor in the mitochondrial alteration and apoptotic proneness of cells from HD patients: the glycoshingolipid raft-like microdomains. In fact, we have previously shown that mitochondrial raft-like microdomains play a role in the mitochondrial morphogenetic remodeling associated with cell death, contributing to the recruitment of fission-associated molecules and to the modifications of mitochondrial curvature
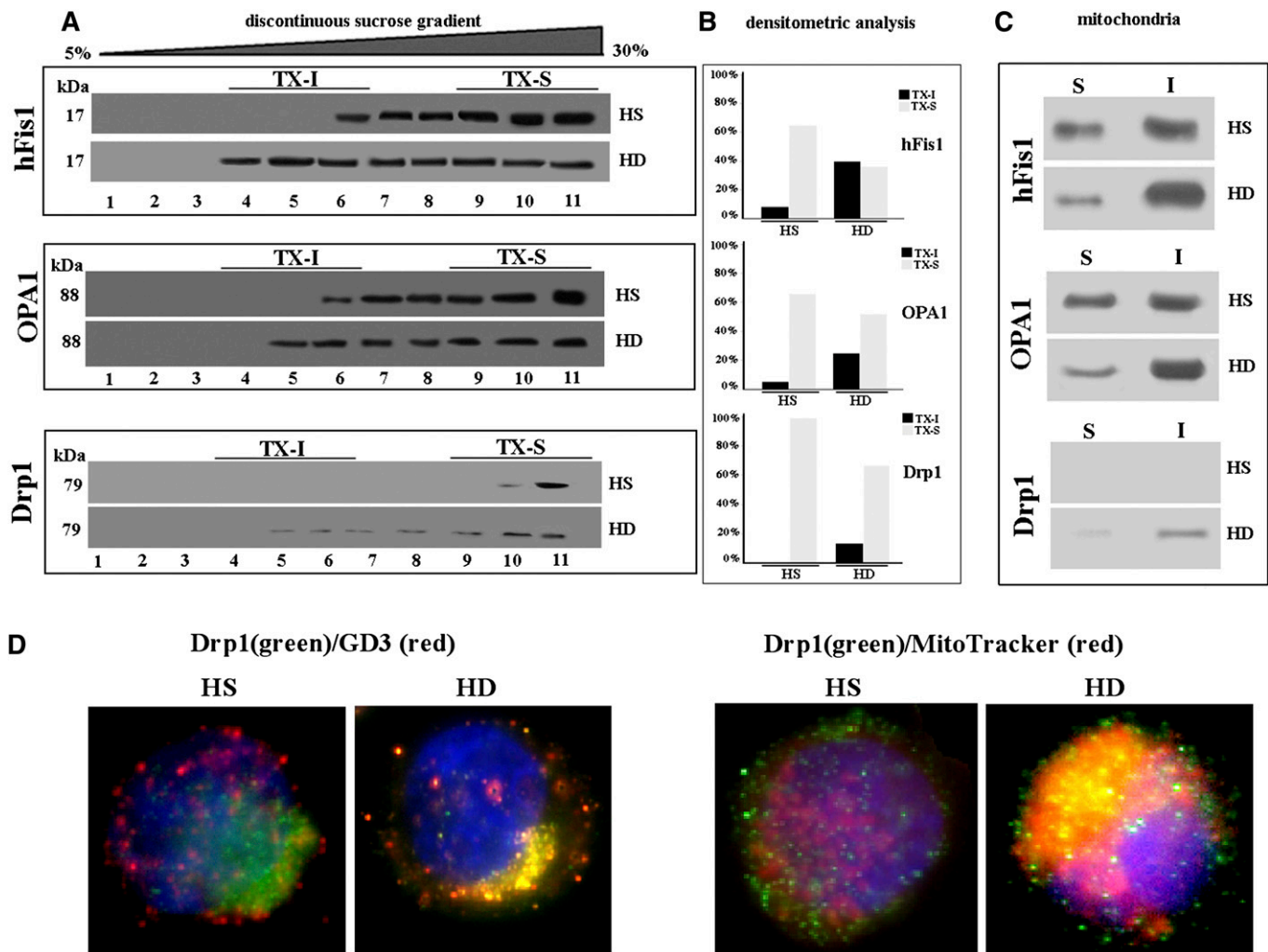
Fig. 5. Mitochondrial fission machinery. A: Western blot analysis of sucrose gradient fractions. Cells from HD patients or HS were lysed, and the supernatant fraction was subjected to sucrose density gradient. After centrifugation, the gradient was fractioned, and each gradient fraction was recovered and analyzed by Western blot. First line: fractions obtained after sucrose density gradient, either HD or HS cells, were analyzed using an anti-hFis1 polyclonal Ab. Second line: fractions obtained after sucrose density gradient, either HD or HS cells, were analyzed using an anti-OPA1 MoAb. Third line: fractions obtained after sucrose density gradient, either HD or HS cells, were analyzed using an anti-Drp1 MoAb. B: Densitometric analysis of sucrose gradient fractions. The columns indicate the percent distribution across the gel of fractions 4, 5, and 6 (buoyant low-density TX-100-resistant, TX-I) and 9, 10, and 11 (TX-100-soluble fractions, TX-S), as detected by densitometric scanning analysis. C: Mitochondria from HD or HS cells were detergent solubilized as reported in Materials and Methods. Both Triton X-100-soluble (S) and -insoluble (I) fractions were analyzed by Western blot and probed with anti-hFis1 polyclonal Ab, anti-OPA1 MoAb, and anti-Drp1 MoAb. The fraction samples were loaded by volume. D: Immunofluorescence analysis after cell double staining with MitoTracker Red/anti-Drp1 (right panel) or with anti-GD3/anti-Drp1 shows that GD3 and Drp1 colocalize at the mitochondrial level in HD cells only. The yellow fluorescence areas indicate the colocalization.

necessary for mitochondrial fission dynamics (36–38). We show herein that Htt was present in mitochondria and associated in mitochondrial lipid microdomains in cells from HD patients, but not in cells from HS. Furthermore, the distribution of key molecules involved in the mitochondrial fission machinery (26–28) was found to be deeply altered in cells from HD patients in comparison to control cells from HS. For instance, Drp1 was constitutively localized in raft-like microdomains in cells from HD patients. Altogether, these findings suggest that microdomains could "engulf" fission-associated molecules and associate with mutated Htt, giving rise to a multimolecular complex affecting mitochondrial fate. In addition, however, we cannot rule out the possibility that this association

could participate in mitochondrial redistribution in the cell cytoplasm. In fact, as previously shown (39), the organelles appear to lose their typical random distribution in cells from HD patients and to form large clusters and macro-aggregates. We can hypothesize that the association formed by microdomains, fission molecules, and Htt could act as a sort of "adhesive device," leading to the striking aggregations of mitochondria detectable in lymphoid cells from HD patients. On the basis of the literature (35), we cannot exclude that this multimolecular complex and related disturbances of mitochondria integrity could also impair mitochondria-mediated cell function in neuronal cells.

These hypotheses are substantiated by the experiments carried out in the presence of FB1, a ceramide synthase
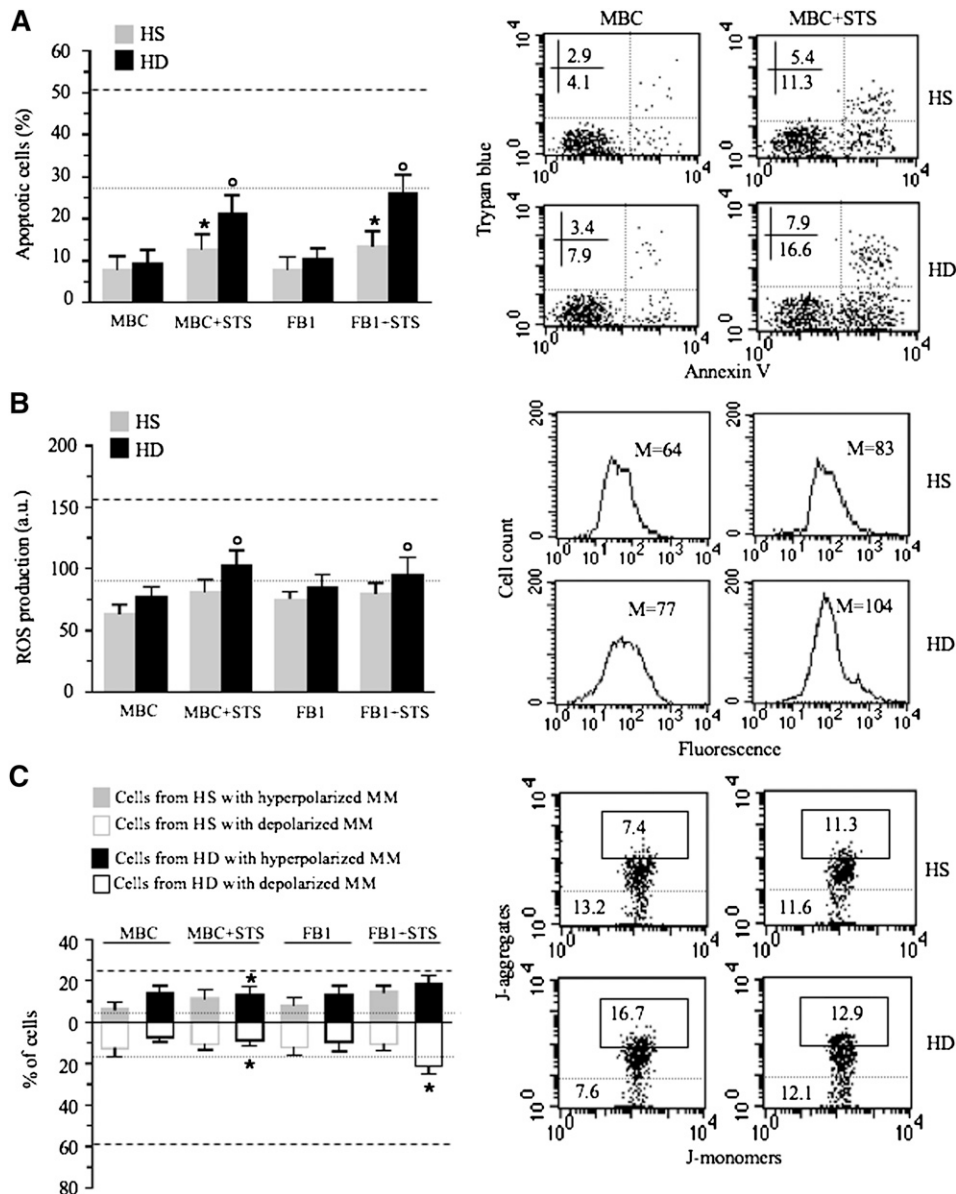
Fig. 6. Mitochondrial raft-like microdomains and apoptotic susceptibility. A: Biparametric flow cytometry analysis of apoptosis after double staining of cells with annexin V-FITC/Trypan blue. In the left panel, bar graph shows the results obtained from three independent experiments reported as mean ± SD. * $P < 0.01$ cells treated with MBC+STS or FB1+ STS versus cells from HS treated with STS; ° $P < 0.01$ cells treated with MBC+STS or FB1+ STS versus cells from HD patients treated with STS. In the right panels, dot plots from a representative experiment are shown. Numbers represent the percentage of annexin V single-positive cells (early apoptosis, lower right quadrant) or annexin V/Trypan blue double-positive cells (late apoptosis, upper right quadrant). B: Cytofluorimetric analysis of superoxide anion production. Reported values represent the median fluorescence. In the left panel, bar graph shows the results obtained from three independent experiments reported as mean ± SD. ° $P < 0.01$ cells treated with MBC+STS versus cells from HD patients treated with STS; ° $P < 0.01$ cells treated with FB1+STS versus cells from HD patients treated with STS. In the right panels, results obtained in a representative experiment are shown as fluorescence emission histograms. Dotted lines in left panels indicate values found in HS cells treated with STS, whereas dashed lines indicate values found in HD cells treated with STS (corresponding to data reported in Fig. 1). C: Biparametric flow cytometry analysis of MMP after staining with JC-1. In the left panel, bar graph shows the results obtained from three independent experiments reported as mean ± SD. Full and empty columns represent the percentages of cells with hyperpolarized (MMH) or depolarized (MMD) mitochondrial membrane, respectively. * $P < 0.01$ cells treated with MBC+STS versus cells from HD patients treated with STS; * $P < 0.01$ cells treated with FB1+STS versus cells from HD patients treated with STS. In the right panels, dot plots from a representative experiment are shown. Numbers reported in the boxed area represent the percentages of cells with hyperpolarized mitochondria. In the area under the dotted line, the percentage of cells with depolarized mitochondria is reported. Results obtained in a representative experiment are shown.

inhibitor (29, 30), and MBC, a raft disruptor (13, 31). Both of these agents are capable of impairing the peculiar mitochondrial remodeling occurring in cells from HD patients, i.e., redistribution and aggregation as well as MMP changes. A decreased apoptotic susceptibility was also detected in the presence of FB1 and MBC. These observations are in line with our previous studies demonstrating that in HD cells, the fragmented mitochondria are characterized by cristae alterations that are aggravated by apoptotic stimulation and can be corrected by maneuvers that prevent fission and cristae remodelling (32, 39). Finally, as concerns hyperpolarization of MM detected in cells from HD patients, this could represent a sort of "risk factor," also contributing to the high apoptotic susceptibility of these cells (39). Increased MMP is probably caused by a mechanism associated with the generation of ROS/nitrogen species, as suggested by other authors (40). Accordingly, in cells from HD patients, ROS generation measured by DHE was found to be constitutively higher than in HS cells, irrespective of any proapoptotic stimulation.

Altogether, these observations support the idea that raft-like microdomains could take part to the mitochondrial impairment occurring in cells from HD patients. This is in line with very recent observations claiming emerging roles of cholesterol in HD (41, 42). In fact, alterations in cholesterol homeostasis have also been detected in several experimental models of HD (43). Because lipid rafts are enriched in sphingolipids (44) and because cholesterol interacts preferentially, although not exclusively, with sphingolipids due to their structure and the saturation of the hydrocarbon chains, raft-like microdomains generally contain 3- to 5-fold the amount of cholesterol found in the surrounding bilayer (45). Hence, we can suggest that mitochondrial raft-like microdomains could represent a key contributor to the pathophysiology of HD. For instance, nontoxic semisynthetic cyclodextrins, which are widely used in vitro and in vivo as drug carriers, including in preclinical studies on HD (46), could be taken into consideration for their raft-targeted activity. Hence, on the basis of the results reported above, molecularly targeted therapy inhibiting the interaction of Htt and Drp1 with mitochondrial raft-like microdomains may decrease mitochondrial fragmentation and aggregate formation.

In conclusion, the present report suggests that lymphoblastoid cells from HD patients can provide useful information as concerns subcellular abnormalities described in the peripheral blood lymphocytes of HD patients (47), but more generally, they can also represent a useful tool in studies aimed at deciphering the complex framework of pathogenetic events occurring in cells of HD patients.

REFERENCES

1. Li, S. H., and X. J. Li. 2004. Huntingtin and its role in neuronal degeneration. *Neuroscientist.* **10:** 467–475.
2. Squitieri, F., C. Gellera, M. Cannella, C. Mariotti, G. Cislaghi, D. C. Rubinsztein, E. W. Almqvist, D. Turner, A. C. Bachoud-Levi, S. A. Simpson, et al. 2003. Homozygosity for CAG mutation in Huntington disease is associated with a more severe clinical course. *Brain.* **126:** 946–955.
3. DiFiglia, M., E. Sapp, K. O. Chase, S. W. Davies, G. P. Bates, J. P. Vonsattel, and N. Aronin. 1997. Aggregation of huntington in neuronal intranuclear inclusions and dystrophic neurites in brain. *Science.* **277:** 1990–1993.
4. Sawa, A. 2001. Mechanisms for neuronal cell death and dysfunction in Huntington's disease: pathological cross-talk between the nucleus and the mitochondria? *J. Mol. Med.* **79:** 375–381.
5. Cui, L., H. Jeong, F. Borovechi, C. N. Parkhurst, N. Tanese, and D. Kraic. 2006. Transcriptional repression of PGC-1alpha by mutant huntingtin leads to mitochondrial dysfunction and neurodegeneration. *Cell.* **127:** 59–69.
6. Panov, A. V., C. A. Gutekunst, B. R. Leavitt, M. R. Hayden, J. R. Burke, W. J. Strittmatter, and J. T. Greenamyre. 2002. Early mitochondrial calcium defects in Huntington's disease are a direct affect of polyglutamines. *Nat. Neurosci.* **5:** 731–736.
7. Yu, Z. X., S. H. Li, J. Evans, A. Pillarisetti, H. Li, and X. J. Li. 2003. Mutant huntingtin causes context-dependent neurodegeneration in mice with Huntington's disease. *J. Neurosci.* **23:** 2193–2202.
8. Iwata, A., B. E. Riley, J. A. Johnston, and R. R. Kopito. 2005. HDAC6 and microtubules are required for autophagic degradation of aggregated Huntingtin. *J. Biol. Chem.* **280:** 40282–40292.
9. Kroemer, G., W. S. El-Deiry, P. Golstein, M. E. Peter, D. Vaux, P. Vandenabeele, B. Zhivotovsky, M. V. Blagosklonny, W. Malorni, N. A. Knight, et al. 2005. Classification of cell death: recommendations of the Nomenclature Committee on Cell Death. *Cell Death Differ.* **12:** 1463–1467.
10. Cuervo, A. M. 2010. The plasma membrane brings autophagosomes to life. *Nat. Cell Biol.* **12:** 735–737.
11. Sawa, A., G. W. Wiegand, J. Cooper, R. L. Margolis, A. H. Sharp, J. F. Lawler, Jr., J. T. Greenamyre, S. H. Snyder, and C. A. Ross. 1999. Increased apoptosis of Huntington disease lymphoblasts associated with repeat length-dependent mitochondrial depolarization. *Nat. Med.* **5:** 1194–1198.
12. Nagata, E., A. Sawa, C. A. Ross, and S. H. Snyder. 2004. Autophagosome-like vacuole formation in Huntington's disease lymphoblasts. *Neuroreport.* **15:** 1325–1328.
13. Garofalo, T., A. M. Giammarioli, R. Misasi, A. Tinari, V. Manganelli, L. Gambardella, A. Pavan, W. Malorni, and M. Sorice. 2005. Lipid microdomains contribute to apoptosis-associated modifications of mitochondria in T cells. *Cell Death Differ.* **12:** 1378–1389.
14. Ciarlo, L., V. Manganelli, T. Garofalo, P. Matarrese, A. Tinari, R. Misasi, W. Malorni, and M. Sorice. 2010. Association of fission proteins with mitochondrial raft-like domains. *Cell Death Differ.* **17:** 1047–1058.
15. Sorice, M., P. Matarrese, V. Manganelli, A. Tinari, A. M. Giammarioli, V. Mattei, R. Misasi, T. Garofalo, and W. Malorni. 2010. Role of GD3-CLIPR-59 association in lymphoblastoid T cell apoptosis triggered by CD95/Fas. *PLoS ONE.* **5:** e8507.
16. Peshavariya, H. M., G. J. Dusting, and S. Selemidis. 2007. Analysis of dihydroethidium fluorescence for the detection of intracellular and extracellular superoxide produced by NADPH oxidase. *Free Radic. Res.* **41:** 699–712.
17. Cossarizza, A., C. Franceschi, D. Monti, S. Salvioli, E. Bellesia, R. Rivabene, L. Biondo, G. Rainaldi, A. Tinari, and W. Malorni. 1995. Protective effect of N-acetylcysteine in tumor necrosis factor-alpha-induced apoptosis in U937 cells: the role of mitochondria. *Exp. Cell Res.* **220:** 232–240.
18. Zamzami, N., C. Maisse, D. Metivier, and G. Kroemer. 2001. Measurement of membrane permeability and permeability transition of mitochondria. *Methods Cell Biol.* **65:** 147–158.
19. Skibbens, J. E., M. G. Roth, and K. S. Matlin. 1989. Differential extractability of influenza virus hemagglutinin during intracellular transport in polarized epithelial cells and nonpolar fibroblasts. *J. Cell Biol.* **108:** 821–832.
20. Malorni, W., T. Garofalo, A. Tinari, R. Misasi, and M. Sorice. 2008. Analyzing lipid rafts dynamics during cell apoptosis. *Methods Enzymol.* **442:** 125–140.
21. Nicotera, P., M. Leist, and E. Ferrando-May. 1999. Apoptosis and necrosis: different execution of the same death. *Biochem. Soc. Symp.* **66:** 69–73.
22. Choi, K., J. Kim, G. W. Kim, and C. Choi. 2009. Oxidative stress-induced necrotic cell death via mitochondira-dependent burst of reactive oxygen species. *Curr. Neurovasc. Res.* **6:** 213–222.
23. Carrozzo, R., T. Rizza, A. Stringaro, R. Pierini, E. Mormone, F. M. Santorelli, W. Malorni, and P. Matarrese. 2004. Maternally-inherited Leigh syndrome-related mutations bolster mitochondrial-mediated apoptosis. *J. Neurochem.* **90:** 490–501.

24. Galluzzi, L., N. Zamzami, T. de La Motte Rouge, C. Lemaire, C. Brenner, and G. Kroemer. 2007. Methods for the assessment of mitochondrial membrane permeabilization in apoptosis. *Apoptosis.* **12:** 803–813.

25. Milakovic, T., and G. V. Johnson. 2005. Mitochondrial respiration and ATP production are significantly impaired in striatal cells expressing mutant huntingtin. *J. Biol. Chem.* **280:** 30773–30782.

26. Bossy-Wetzel, E., M. J. Barsoum, A. Godzik, R. Schwarzenbacher, and S. A. Lipton. 2003. Mitochondrial fission in apoptosis, neurodegeneration and aging. *Curr. Opin. Cell Biol.* **15:** 706–716.

27. Jahani-Asl, A., K. Pilon-Larose, W. Xu, J. G. MacLaurin, D. S. Park, H. M. McBride, and R. S. Slack. 2011. The mitochondrial inner membrane GTPase, optic atrophy 1 (Opa1), restores mitochondrial morphology and promotes neuronal survival following excitotoxicity. *J. Biol. Chem.* **286:** 4772–4782.

28. Pitts, K. R., Y. Yoon, E. W. Krueger, and M. A. McNiven. 1999. The dynamin-like protein DLP1 is essential for normal distribution and morphology of the endoplasmic reticulum and mitochondria in mammalian cells. *Mol. Biol. Cell.* **10:** 4403–4417.

29. Marasas, W. F., R. T. Riley, K. A. Hendricks, V. L. Stevens, T. W. Sadler, J. Gelineau-van Waes, S. A. Missmer, J. Cabrera, O. Torres, W. C. Gelderblom, et al. 2004. Fumonisins disrupt sphingolipid metabolism, folate transport, and neural tube development in embryo culture and in vivo: a potential risk factor for human neural tube defects among populations consuming fumonisin-contaminated maize. *J. Nutr.* **134:** 711–716.

30. Sjögren, B., and P. Svenningsson. 2007. Depletion of the lipid raft constituents, sphingomyelin and ganglioside, decreases serotonin binding at human 5-HT7(a) receptors in HeLa cells. *Acta Physiol. (Oxf.).* **190:** 47–53.

31. Xing, Y., Y. Gu, L. C. Xu, C. A. Siedlecki, H. J. Donahue, and J. You. 2011. Effects of membrane cholesterol depletion and GPI-anchored protein reduction on osteoblastic mechanotransduction. *J. Cell. Physiol.* **226:** 2350–2359.

32. Costa, V., M. Giacomello, R. Hudec, R. Lopreiato, G. Ermak, D. Lim, W. Malorni, K. J. Davies, E. Carafoli, and L. Scorrano. 2010. Mitochondrial fission and cristae disruption increase the response of cell models of Huntington's disease to apoptotic stimuli. *EMBO Mol. Med.* **12:** 490–503.

33. Squitieri, F., V. Maglione, S. Orobello, and F. Fornai. 2011. Genotype-aging-dependent abnormal caspase activity in Huntington disease blood cells. *J. Neural Transm.* **118:** 1599–1607.

34. Reddy, P. H., and U. P. Shirendeb. 2012. Mutant huntingtin, abnormal mitochondrial dynamics, defective axonal transport of mitochondria, and selective synaptic degeneration in Huntington's disease. *Biochim. Biophys. Acta.* **1822:** 101–110.

35. Shirendeb, U. P., M. J. Calkins, M. Manczak, V. Anekonda, B. Dufour, J. L. McBride, P. Mao, and P. H. Reddy. 2012. Mutant huntingtin's interaction with mitochondrial Drp1 impairs mitochondrial biogenesis and causes defective axonal transport and synaptic degeneration in Huntington's disease. *Hum. Mol. Genet.* **21:** 406–420.

36. Wells, R. C., and R. B. Hill. 2011. The cytosolic domain of Fis1 binds and reversibly clusters lipid vesicles. *PLoS ONE.* **6:** e21384.

37. Lucken-Ardjomande, S., S. Montessuit, and J. C. Martinou. 2008. Contributions to Bax insertion and oligomerization of lipids of the mitochondrial outer membrane. *Cell Death Differ.* **15:** 929–937.

38. Reddy, P. H., P. Mao, and M. Manczak. 2009. Mitochondrial structural and functional dynamics in Huntington's disease. *Brain Res. Rev.* **61:** 33–48.

39. Mormone, E., P. Matarrese, A. Tinari, M. Cannella, V. Maglione, M. G. Farrace, M. Piacentini, L. Frati, W. Malorni, and F. Squitieri. 2006. Genotype-dependent priming to self- and xeno-cannibalism in heterozygous and homozygous lymphoblasts from patients with Huntington's disease. *J. Neurochem.* **98:** 1090–1099.

40. Nagy, G., M. Barcza, N. Gonchoroff, P. E. Phillips, and A. Perl. 2004. Nitric oxide-dependent mitochondrial biogenesis generates Ca2+ signaling profile of lupus T cells. *J. Immunol.* **173:** 3676–3683.

41. Valenza, M., and M. Cattaneo. 2011. Emerging roles for cholesterol in Huntington's disease. *Trends Neurosci.* **34:** 474–486.

42. Karasinska, J. M., and M. R. Hayden. 2011. Cholesterol metabolism in Huntington disease. *Nat Rev Neurol.* **7:** 561–572.

43. del Toro, D., X. Xifró, A. Pol, S. Humbert, F. Saudou, J. M. Canals, and J. Alberch. 2010. Altered cholesterol homeostasis contributes to enhanced excitotoxicity in Huntington's disease. *J. Neurochem.* **115:** 153–167.

44. Sorice, M., T. Garofalo, R. Misasi, V. Manganelli, R. Vona, and W. Malorni. 2012. Ganglioside GD3 as a RAFT component in cell death regulation. *Anticancer. Agents Med. Chem.* **12:** 376–382.

45. Malorni, W., A. M. Giammarioli, T. Garofalo, and M. Sorice. 2007. Dynamics of lipid rafts components during lymphocyte apoptosis: the paradigmatic role of GD3. *Apoptosis.* **12:** 941–949.

46. Hockly, E., V. M. Richon, B. Woodman, D. L. Smith, X. Zhou, E. Rosa, K. Sathasivam, S. Ghazi-Noori, A. Mahal, P. A. Lowden, et al. 2003. Suberoylanilide hydroxamic acid, a histone deacetylase inhibitor, ameliorates motor deficits in a mouse model of Huntington's disease. *Proc. Natl. Acad. Sci. USA.* **100:** 2041–2046.

47. Sassone, J., C. Colciago, G. Cislaghi, V. Silani, and A. Ciammola. 2009. Huntington's disease: the current state of research with peripheral tissues. *Exp. Neurol.* **219:** 385–397.